

TECHNICAL UNIVERSITY OF CRETE



School of Production Engineering & Management

DIPLOMA THESIS

Local Ramp Metering: Linear Quadratic Integral
Regulator for Distant Downstream Bottlenecks

By Stylianopoulou Evgenia

*Thesis submitted in partial fulfilment of the requirements
for the degree of Diploma in Production Engineering and Management*

Advisor: Prof. Papageorgiou Markos

Chania, Crete, 2018

The present thesis is approved by the following jury:

Thesis Committee:

Markos Papageorgiou (Advisor)

Professor, School of Production Engineering and Management
Technical University of Crete, Chania, Greece

Ioannis Papamichail

Associate Professor, School of Production Engineering and Management
Technical University of Crete, Chania, Greece

Anargiros Delis

Associate Professor, School of Production Engineering and Management
Technical University of Crete, Chania, Greece

Acknowledgements

I would like to express my very great appreciation to Prof. Markos Papageorgiou for his valuable and constructive suggestions during the planning and development of this research work and for trusting me as a member of the Dynamic Systems and Simulation Laboratory. I would also like to extend my thanks to Prof. Ioannis Papamichail for his advice and assistance in keeping my progress on schedule. I would also like to thank Prof. Anargiros Delis for accepting to be a member of this thesis committee.

Furthermore, I am thankful to Maria Kontorinaki, member of the Dynamic Systems and Simulation Laboratory, for her help in offering me the resources for this research, her patience, her valuable knowledge and guidance during my first steps in the laboratory. I would also like to extend my thanks to the members of the Dynamic Systems and Simulation Laboratory for their help in offering me their advice and suggestions during the planning and development of this research work.

Finally, I must express my very profound gratitude to my parents, my sister and my partner, Konstantinos for providing me with unfailing support and continuous encouragement throughout my years of study and through the process of researching and writing this thesis. This accomplishment would not have been possible without them.

Abstract

Ramp Metering (RM) is one of the most effective control measures applied in freeways. RM, when driven by an opportune control strategy, alleviates significantly the overall traffic congestion and improves freeway conditions in terms of safety, travel time and reliability.

Local ramp metering strategies are implemented for a single ramp and compute the metering rates by taking into account traffic conditions in the vicinity of a ramp. Several real-time ramp metering control algorithms have been developed and proposed in the literature, with ALINEA, an I-type feedback regulator, being the most popular and efficient as it has already been implemented in many field applications. However, there exist cases where bottlenecks with smaller capacity, than the merging area's, exist further downstream due to, for example, a lane drop, a tunnel, an upgrade, a speed limit area or an uncontrolled downstream on-ramp. In such cases, ALINEA fails to respond satisfactorily and, therefore, other control strategies should be employed, which have been designed so as to use measurements from those further downstream areas where the bottleneck is activated.

Towards this direction, this work investigates the application of a new control strategy, specifically a Linear Quadratic Regulator augmented with integral action (LQI), for the local ramp metering control problem when bottlenecks are located many kilometres (up to 5 km) downstream of the metered on-ramp. LQI makes use of measurements all along the area extending from the controllable on-ramp to the bottleneck location, being therefore capable to improve the stability and robustness properties of the control loop.

This study investigates various downstream bottleneck scenarios and uses the second-order macroscopic traffic flow model METANET as ground truth for the control application. Simulation results revealed that: i) the proposed methodology handles efficiently the local RM task in case of very distant downstream bottlenecks and, ii) LQI is less sensitive compared to previously proposed control strategies.

Contents

ACKNOWLEDGEMENTS	5
ABSTRACT.....	7
CONTENTS	9
LIST OF FIGURES	12
LIST OF TABLES	13
1. INTRODUCTION	15
1.1 MOTIVATION AND THESIS OBJECTIVES	15
1.2 THESIS OUTLINE.....	17
2. THEORETICAL BACKGROUND.....	19
2.1 CONTROL THEORY	19
2.1.1 Control Loop.....	20
2.1.2 Stability, Controllability and Observability.....	20
2.2 TRAFFIC FLOW CONTROL	21
2.2.1 Variable Speed Limits (VSL)	21
2.2.2 Route Guidance.....	22
2.2.3 Ramp Metering (RM).....	22
2.3 RAMP METERING CONTROL STRATEGIES	24
2.3.1 Existing local RM Strategies.....	25
2.4 TRAFFIC FLOW MODELING.....	26
2.4.1 METANET Traffic Flow Model.....	29
2.4.2 Description of stretch.....	30

2.4.3 <i>Fundamental Diagram</i>	32
3. LQI REGULATOR	35
3.1 INTRODUCTION	35
3.2 LQI FORMULATION.....	35
4. LOCAL RAMP METERING USING LQI	39
4.1 SIMULATION MODEL AND SIMULATION SET-UP.....	39
4.1.1 <i>Network Description</i>	39
4.1.2 <i>Fundamental Diagram and Demand scenarios</i>	41
4.2 CONTROL SET-UP.....	43
5. SIMULATION INVESTIGATIONS.....	45
5.1 SET POINT SELECTION.....	45
5.2 SIMULATION INVESTIGATIONS- BOTTLENECK CASE 1	48
5.3 SIMULATION INVESTIGATIONS- BOTTLENECK CASE 2	50
5.4 SIMULATION INVESTIGATIONS- BOTTLENECK CASE 3	52
5.5 SIMULATION INVESTIGATIONS- BOTTLENECK CASE 4.....	54
5.6 SIMULATION INVESTIGATIONS- BOTTLENECK CASE 5.....	56
5.7 CONSTANT GAINS.....	59
5.8 CONTROL DECISION.....	59
6. CONCLUSION AND FUTURE WORK	61
REFERENCES	ERROR! BOOKMARK NOT DEFINED.

List of Figures

Figure 1: Description of a control loop	19
Figure 2: Hypothetical Stretch	30
Figure 3: Flow-Density diagram.....	33
Figure 4: Bottleneck case1.....	40
Figure 5: Bottleneck case 2.....	40
Figure 6: Bottleneck case 3.....	40
Figure 7: Bottleneck case 4.....	40
8: Bottleneck case 5	41
Figure 9: Fundamental diagrams considered	41
Figure 10: Utilized mainstream and on-ramp demand scenarios.....	42
Figure 11: Bottleneck case 1: (a) No control case, (b) control case with LQI, (c) control case with PI-ALINEA	48
Figure 12: Bottleneck case 2: (a) No control case, (b) control case with LQI, (c) control case with PI-ALINEA	50
Figure 13: Bottleneck case 3: (a) No control case, (b) control case with LQI, (c) control case with PI-ALINEA	52
Figure 14: Bottleneck case 4: (a) No control case, (b) control case with LQI, (c) control case with PI-ALINEA	54
Figure 15: Bottleneck case 5 : (a) No control case, (b) control case with LQI, (c) control case with PI-ALINEA	56
Figure 16: Control decision for each bottleneck case	60

List of Tables

Table 1: Set-point selection	46
Table 2: Gain values for each bottleneck case.....	47
Table 3: Improvement of stationary flow	58

1. Introduction

This first section corresponds to the introductory section of this thesis. Sections 1.1 describes the motivations and objectives of this work, while Section 1.2 presents the outline of this thesis.

1.1 Motivation and Thesis Objectives

The number of vehicles and the need of transportation is continuously growing causing traffic congestion problems. The continuously increasing daily traffic congestion on freeway networks around the world calls for innovative control measures and control strategies that would drastically improve the current traffic conditions [1], [2]. Traffic congestion in freeways has become a common phenomenon, which leads to delays, lower speeds, long trip times, increased vehicular queueing, increased fuel consumption, reduced traffic security and severe air pollution. As traffic demand approaches the available capacity of the freeway, traffic congestion appears and bottleneck areas start to activate. A traffic bottleneck is a localized disruption of vehicular traffic on a freeway caused mainly due to the existence of lane drops, bridges, tunnels, upgrades, curvatures, speed limit areas and uncontrollable ramps. In order to avoid congestion phenomena, several control measures and control strategies have been proposed [17].

In order to deal with the traffic congestion problems in freeways, there have been many methods developed and proposed in literature during the last years [12], [15]. Related studies provide methods, which guarantee strong theoretical properties and are easily applicable for real traffic control. Thus, Ramp Metering (RM) can be defined as a method by which a traffic flow to gain access to a freeway network, is controlled at the access point via traffic signals. This control aims at maximize the capacity of the freeway and prevent the congestion phenomena. As far as RM is

concerned, several RM control strategies have been proposed in the literature, with ALINEA [19], an I-type feedback regulator, being the most popular and efficient. ALINEA aims to maximize freeway throughput in the ramp merging area and, to this end, occupancy measurements are required and have to be collected from a mainstream cross section located at most a few hundred meters downstream of the metered on-ramp. Another control strategy have been proposed is PI-ALINEA (Proportional Integral) [10], an extension of ALINEA, that instead of using measurements from the merging area, takes the measurements from the downstream bottlenecks [9]. PI-ALINEA is proposed because of the main weakness of ALINEA regulator that compute the control law only on the basis of measurements at the region that the control action is actuated. According to the ones mentioned before, areas with smaller capacity than the merging area may exist further downstream of the freeway. PI-ALINEA seems to be efficient in cases where areas with smaller capacity than the merging area may exist downstream of the freeway (up to 2 km). Although, PI-ALINEA's action fails in the case of very very far downstream bottlenecks (more than 2 km).

The fact that other strategies, such as PI-ALINEA, fail to succeed handling the control task in these areas, has been a motive to construct a new regulator based on a promising control strategy. This thesis is based on a traffic-responsive ramp metering control algorithm that has been developed to control the ramp locally. Thus, this report aims to present a promising approach for developing a control strategy that is more efficient and robust than the strategies that have been already developed [12], [15].

The proposed control strategy consists of a Linear Quadratic Regulator with Integral action (LQI) in cases where the bottleneck is located many kilometers downstream from the on-ramp (more than 2 km) [6], [8], [31]. In order to test this strategy, various scenarios have been constructed depending on the location of the bottleneck (five scenarios are presented herein) and a freeway with a single on-ramp is assumed. Given the ability of second-order models, this thesis examines the formulation of a popular second-order model, namely METANET [5], [8] [30] model.

This thesis, utilizes mathematical tools that describe general traffic systems and freeways. To summarize, the scope of this work is to test the robustness, the efficiency and the ability of the LQI strategy to handle with success the control task in areas far downstream of the on-ramp's location.

1.2 Thesis Outline

This diploma thesis is composed of 6 Chapters. *Chapter 2* presents briefly some theoretical background issues related to control theory (control loop, stability, controllability and observability). An overview of traffic flow control is also presented (control measures and control strategies). At the end of Chapter 2, there is an introduction in Traffic Flow Modeling and especially the second order METANET model. In Chapter 3, there is a presentation of the build and the formulation of Linear Quadratic Integral regulator. Chapter 4 consist of a description of the simulation set-up and the control set-up used for simulations. In Chapter 5, simulation investigations are presented and compared to other related studies. Finally, Chapter 6 summarizes the conclusions and proposes future work.

2. Theoretical Background

2.1 Control Theory

Control theory deals with the control of continuously operating dynamical systems in freeways, by developing a controller with the appropriate behavior. In order to handle deviations from a desired system behavior, the main tool is the use of feedback. Feedback control theory involves the analysis and synthesis of feedback controllers that manipulate system inputs to obtain a desired effect on the output of the system in the face of system uncertainty and system disturbances.

Sensors deployed in freeways collect information, for designed time steps, about the stationary flow, the mean speed and the density (actual values) of the vehicles. A controller compares actual and desired values (y^* - set point) of the variable of interest and calculates the difference between them (error). Error is applied as feedback to generate a control action in order to make actual and desired values equal. The mathematical background of the process is the system function that express the relation between the input ($u(k)$) and output ($x(k)$) based on the differential equations describing the system (Figure 1).

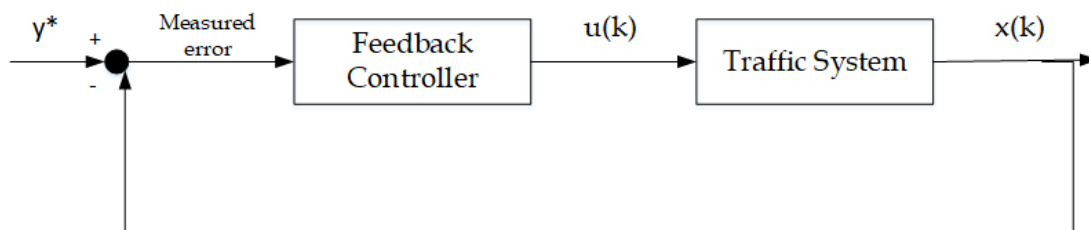


Figure 1: Description of a control loop

2.1.1 Control Loop

There are two types of control loops: *open loop* control and *closed loop* control. In *open loop* control, the control action from the controller is independent of the variable of interest. In *closed loop* control, the control action from the controller is dependent on feedback from the process in the form of the variable of interest. A closed loop controller, that is concerned here, has a feedback loop. It is also called feedback controller.

In general, the kernel of the closed control loop is the control strategy, whose task is to specify in real time the control inputs, based on available measurements in order to achieve the pre-specified goals despite the influence of various disturbances. If a human operator undertakes this task, we have a manual control system. In an automatic control system, this task is undertaken by an algorithm (the control strategy). The relevance and efficiency of the control strategy determines the efficiency of the overall control system. In this thesis a single-input-single-output (SISO) control system is used.

2.1.2 Stability, Controllability and Observability

The task of the control theory is to decide which is the best control strategy to be applied or whether it is even possible to control or stabilize the system. Before that, it is necessary to check if the system is *stabilizable*, *controllable* and *observable*.

Stability of a linear system can be achieved if the poles of its transfer function have negative-real values, the real part of each pole must be less than zero.

Controllability is an important property of a control system. It is related to the possibility of forcing the system into a particular state by using an appropriate control signal. If a state is not controllable, then no signal will ever be able to control the state. If a state is not controllable, but its dynamics are stable, then the state is termed stabilizable.

Observability is the possibility of observing, through output measurements, the state of the system. If a state is not observable, the controller will never be able to

determine the behavior of the state and hence cannot use it to stabilize the system. If a state cannot be observed it might still be detectable. Controllability and observability of a system are mathematical duals.

2.2 Traffic Flow Control

Traffic Flow Control [1], [2] aims to limit congestion phenomena observed at traffic networks, and especially freeway networks. Freeways are congested on a daily basis during rush hours causing congestion that occurs as use increases, and is characterized by slower speeds, longer trip times, and increased vehicular queueing. Thus, the drivers experience delays, the traffic safety is reduced, the fuel consumption and air pollution are increased.

After extensive research, there are control measures have been developed to deal with this phenomenon. Control measures can be used to improve traffic performance. Speed limits, Route guidance and Ramp metering are control measures that are currently applied or could be applied in the near future. Freeway control measures increase the efficiency and safety of the system. To achieve their goal, the following control measures must be driven by appropriate control strategies. The most investigated control measures include:

2.2.1 Variable Speed Limits (VSL)

The working principle of a speed limit system can be categorized based on their intended effects: improving safety, improving traffic flow, or their environmental effects, such as reducing noise or air pollution. VSL offer considerable promise in restoring the credibility of speed limits and improving safety by restricting speeds during adverse conditions. These speed limits change based on road, traffic and weather conditions and they are displayed on the electronic signs in freeways. Traffic sensors along the roadway collect vehicle speeds, congestion information and traffic flow rates to gradually reduce the approaching flow of traffic to the congested

area. Drivers speeding up and slowing down to adjust to the traffic flow. VSL are valuable for traffic safety (reduction of accidents), but their current usage has hardly any positive impact for the increase in throughput or decrease in average travel times.

2.2.2 Route Guidance

Route guidance systems assist drivers in choosing their route when alternative routes exist to their destination. The systems typically display traffic information such as congestion length, the delay on the alternative routes, or the travel time to the next common point on the alternative routes. It is expected to improve the network performance (better use of the available capacity, higher throughput and stability, and less spill-back), and reduce the travel time (minimize delays) for the individual road user as well. Finding the right route guidance configuration is a complex task that should take potentially unfavorable effects and coordination into account.

2.2.3 Ramp Metering (RM)

Ramp Metering is one of the most investigated and applied freeway traffic control measures. A ramp meter is a device, usually a basic traffic light or a two-section signal light together with a signal controller that regulates the flow of traffic entering freeways according to current traffic conditions.

In this thesis, we focus on Ramp Metering as a freeway traffic control measure [18]. By the use of traffic lights positioned at on-ramps, RM reduces overall freeway congestion by managing the amount of traffic entering the freeway. Although, some delay may be caused at waiting ramp queues, the overall time may be decreased due to the optimal operation of the existing infrastructure. Ramp meters on freeways are proved successful in decreasing traffic congestion and improving driver safety.

- **Flow, Reliability and Efficiency**

RM reduces mainstream congestion and overall delay, while increasing flow through the freeway network and traffic throughput. Travel times, even when considering time in queue on the ramp, are generally reduced when ramp metering is implemented. Travel time reliability has become an important measure of ramp metering effectiveness.

- **Safety**

Ramp meters help breaking up platoons of vehicles that are entering the freeway and competing for the same limited gaps in traffic. Thus, RM help to avoid collisions and crashes on the freeway. Effective ramp queue management can prevent queues from spilling into the mainstream flow.

- **Reduced Environmental Impacts**

Ramp meters smooth the traffic flow entering the freeway so vehicles can merge with the mainstream network with minimal disruption to traffic flow. By reducing periods of stop-and-go conditions that caused because of the congestion, vehicle emissions and fuel consumption on the freeway can be reduced.

- **Cost**

To estimate if the implementation of ramp metering is great value, it is necessary to evaluate and compare the cost effectiveness of ramp metering implementation and operation against the no ramp meter scenario. This benefit/cost analysis seems to be excellent for transportation improvements.

In general, without ramp meters in freeways, vehicles merge in packed platoons, causing drivers on the mainstream freeway to slow down or even stop in order to allow to other vehicles to enter the freeway. Thus, the vehicles develop lower speeds, both on the mainstream and on the ramp, and that quickly leads to congestion and sometimes stop-and-go conditions. Ramp meters can control the rates at which vehicles enter the mainstream network from the on ramp. These vehicles enter the mainstream flow smoothly and there is no need any more for vehicles in the mainstream network to reduce speed. In addition, RM help managing the entrance demand at a level that is near the capacity of the freeway, which prevents traffic flow breakdowns. Thus, RM reduce at peak hours the density of the freeway and maximize the flow at the freeway exit [27].

2.3 Ramp Metering Control Strategies

In order to achieve a sustainable mobility system, by taking care the needs of the system, it is necessary to develop a control strategy. The control methods developed nowadays must have the objectives not only of decreasing travel delays experienced by drivers in the traffic system but also of reducing pollution , fuel consumption, accidents, noise and so on. Control measures such as Ramp metering, which described before, must be driven by appropriate control strategies, to achieve their goals. For instance, ramp metering control strategies have as an ultimate goal to determine, in the most efficient way, the inflows from the on-ramps, when congestion phenomena are present at the corresponding mainstream region, so as to maximize the freeway throughput.

In general, control strategies can be classified into *fixed-time* and *traffic-responsive* strategies. Fixed-time control strategies use historical data, while traffic-responsive (real-time) strategies use current traffic data, provided by sensors installed in the freeway network and the on-ramps (traffic measurements). Their goals are to specify the optimal plans that depend on the time of day and to specify the values of the control variables that minimize the extend of congestion, respectively.

Traffic responsive strategies, that interest us, can be classified into *local* and *coordinated* strategies. Local ramp metering strategies are implemented for a single ramp by taking into account traffic conditions within a vicinity of this ramp to compute the metering rates; while coordinated ramp metering strategies determine the metering rates of multiple ramps based on the traffic conditions of a correspondingly extended section of the network. For the purpose of this study, local ramp metering will be considered. Moreover, local ramp metering strategies make use of measurements from further downstream of a single on-ramp. Instead, coordinated ramp metering strategies make use of measurements from the whole region of the network to control all metered ramps of the network.

The most important control strategies include *Nonlinear Optimal Control*, *Model Predictive Control* and *Explicit Feedback Control*. The first two control approaches are very efficient but they are highly demanding from the computational point of view. Explicit feedback control approaches has been shown to enhance the efficiency of traffic operations without the computational effort.

2.3.1 Existing local RM Strategies

There are a wide range of ramp metering control strategies and algorithms [12], [15], [24]. Local control strategies select metering rates based on traffic conditions present on the on ramp and are often used as back-up strategies. When calculating a metering rate, control takes into account traffic conditions upstream and downstream from an individual ramp along a specific freeway segment.

2.3.1.1 ALINEA and PI-ALINEA

ALINEA controls the traffic entering from an on-ramp and targets a critical density in the mainstream merging segment to maximize the freeway throughput. *ALINEA* aims to maximize freeway throughput in the ramp merging area and, to this end, required occupancy measurements should be collected from a mainstream cross

section that is located at most a few hundred meters downstream of the metered on-ramp (where the merging congestion is likely to appear first). This can be achieved by maintaining traffic density in the merging area, around the critical density, so that the mainstream flow of the merging area can be maximized. In some cases, however, a bottleneck with lower capacity than the merging area may exist further downstream, due to the existence of curvatures, lane drops, tunnels or downstream uncontrollable on-ramps. In these cases, density that feeds the feedback ramp metering controller should be collected at the downstream location because the maximum throughput that can be accommodated by the downstream bottleneck is lower than that in the merging area.

PI-ALINEA, as feedback ramp metering strategy, is a functional extension of *ALINEA*. *PI-ALINEA* is very efficient in handling the local ramp metering task in presence of distant downstream bottlenecks. Thus, *PI-ALINEA* acts like *ALINEA*, but it is a suitable proportional-integral extension of *ALINEA* and is selected to investigate such cases [9], [19].

2.4 Traffic flow Modeling

Traffic flow modeling [7] is a branch of mathematics and engineering that studies the relationship between the drivers and their environment. A lot of mathematical models have been proposed since the appearance of traffic jams, in order to describe the traffic flow situation on freeways. These mathematical models, can be used to adjust the traffic flow in crucial areas, maximize the overall throughput of traffic along the stretch of the freeway and as a result solve the traffic jam problem. By these models, we can predict, given certain demand levels, where and when queuing will occur, how long it will take for congestion to resolve, e.t.c. This study is related to the utilization of these mathematical models in developing and testing traffic flow estimation algorithms and traffic control strategies.

The first step in modeling is to study and represent the system by mathematical equations. For the assessment of traffic control strategies, a simulation model is used instead of (or before) a real-world test. Simulation has several advantages because is cheaper and faster than real- world tests and it does not require real human drivers as test subjects.

In general, traffic flow models can be classified as *microscopic*, *macroscopic* or *mesoscopic*, according to the level of detail with which they describe the traffic process [1].

- *Microscopic* traffic flow models describe the behavior of individual vehicles. These models simulate single vehicle-driver units, so the dynamic variables of the models represent microscopic properties like the position and velocity of single vehicles. In microscopic traffic models different characteristics are assigned to each vehicle, such as the driving style of the driver (aggressive, patient), vehicle type (car, truck), destination and route choice. A microscopic model attempts to analyze the flow of traffic by modelling driver-driver and driver-road interactions within a traffic stream which respectively analyzes the interaction between a driver and another driver on road and of a single driver on the different features of a road. In general, it is difficult to calibrate microscopic models with real traffic data because of the large number of the parameters they use. The parameters in macroscopic traffic flow models are less than in microscopic models.
- *Macroscopic* traffic flow models [28] consider the traffic flow as a compressible fluid with well-defined characteristics and describe it with aggregate variables, such as flow, density and mean speed, make use of partial differential equations, a conservation equation and a momentum equation. In macroscopic modeling, under homogeneous traffic conditions in space and time, traffic density is related to traffic volume by a relationship known as the Fundamental Diagram (FD). This relationship provides maximum flow at a

critical density value, while if density is further increased, traffic volume decreases and a, more or less, severe traffic congestion results. Macroscopic traffic flow modeling started when Lighthill and Whitham presented in 1995 a model based on the analogy between traffic flows and flows in rivers. One year later Richards published a similar model. This model is usually referred as the Lighthill-Whitham-Richards (LWR) model [22]. Since then a variety of macroscopic traffic flow models has evolved from the LWR model, with some differences.

- *Mesosopic* traffic flow models, in general, are not used for traffic control and they do not consider the vehicles as individuals. These models describe the behaviour of individual vehicles in probabilistic terms. Examples of these models are headway distribution models and gas-kinetic models.

Moreover, traffic flow models are categorized as *first-order (FOMs)*, *second-order (SOMs)* or *higher-order* models, according to the number of differential equations they include.

- *First-order* models (such as LWR model) are widely known for their simplicity and computational efficiency and this is the reason why they have been used extensively in the past [8]. They include one partial differential equation, which describes the mass conservation law, and consider a static relation between speed and density. Although, they are not able to reproduce the capacity drop phenomenon that is observed at congested freeway areas and the stop-and-go waves that appear at freeway bottlenecks.
- *Second-order* or *higher-order* models (such as Payne model) include except for the conservation equation, one more partial differential equation, which

describes the dynamics of speed and a slightly higher number of parameters, compared to the first-order models.

Another classification of traffic flow models is whether the model is *deterministic* or *stochastic*. *Deterministic* models define the relationship between model inputs, variables, and outputs that describe the behaviour of traffic. *Stochastic* models describe traffic behaviour in terms of relationships between random variables, random reaction time of drivers, randomness in equilibrium speed-density relationships, route choice, etc.

A last classification of traffic flow models is imposed by the *type of mathematical equations* used. The models are described by *Partial Differential Equations (PDEs)*, *Ordinary Differential Equations (ODEs)* or *Difference Equations* (Discrete space-time models).

2.4.1 METANET Traffic Flow Model

METANET that is used in this thesis [5], [30], is a program for motorway network simulation based on a purely macroscopic modelling approach. *METANET* can be applied to existing or hypothetical, multi-origin, multi-destination, multi-route networks with characteristics like on-ramps, off-ramps etc. The fact that is a macroscopic model leads to low computational effort, which is independent of the number of vehicles in the simulated network. This modelling approach allows the simulation of all kinds of traffic conditions and of capacity reducing events. The use of model can be either off-line or in real-time. It is a useful tool to develop and evaluate traffic control strategies, by considering the application of control measures, such as ramp metering. Thus, simulation results by applying *METANET*, are provided in terms of macroscopic traffic variables such as density, flow, speed as well as in terms of travel times. Visualization of the results is provided by time trajectories of selected variables and by graphical representation of the whole network.

2.4.2 Description of stretch

The freeway network is represented by a directed graph. Each stretch has the same geometry and specific characteristics such as on-ramps, off-ramps etc. The simulation of traffic behaviour in the freeway links is macroscopically characterized by the following aggregate variables: *traffic density* ρ (veh/km/lane), *mean speed* v (km/h), and *traffic flow* q (veh/h/lane). For modeling, any considered freeway stretch m is subdivided into a number of N cells with typical lengths L_i of 300 to 800 meters ($i=1, 2, \dots, N$). The time and space arguments are discretized (Figure 2). The time is discretized based on a model time step T (5 – 10 s) and the indexes $k = 1, 2, \dots, N$ at discrete time $t = kT$. The aggregated traffic flow variables are defined for each cell and updated for each model time step.

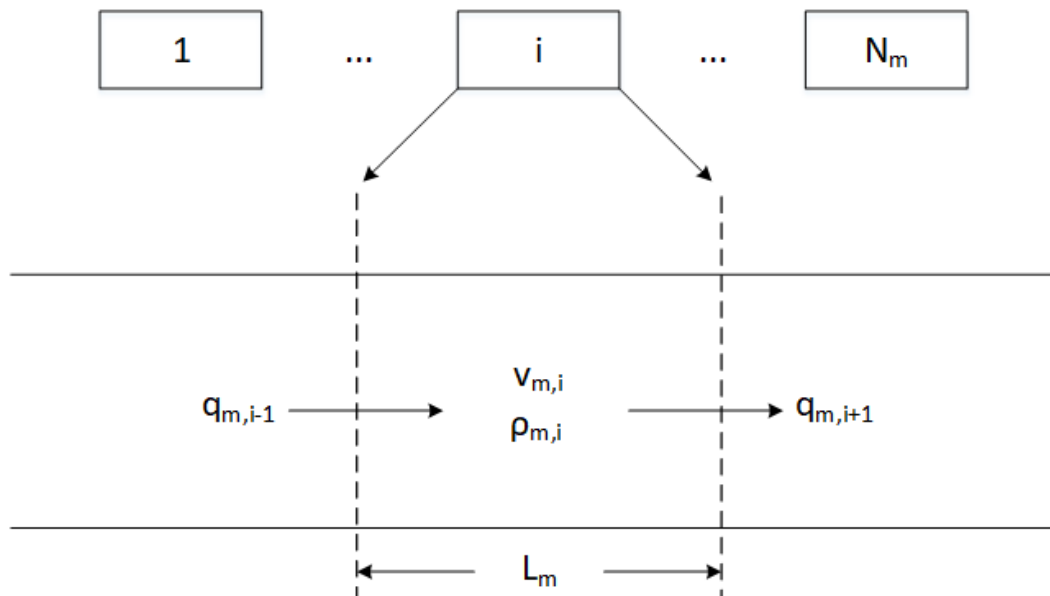


Figure 2: Hypothetical Stretch

Traffic density ρ is the number of vehicles in cell i at time $t = kT$ divided by L_i and by the number of lanes λ_i in the considered stretch m ; mean speed v is the mean speed of vehicles in cell i of stretch m at time $t = kT$; and traffic flow q is the number of

vehicles leaving the cell i of stretch m during the time period $[kT, (k+1)T]$ divided by T (Figure 2).

METANET employs a second-order traffic flow model consisting of two interconnected dynamic equations, which describe the evolution of traffic density and mean speed, respectively. For every stretch m and every cell i , the stochastic nonlinear difference equations of the second-order macroscopic traffic flow model used to calculate the traffic variables are:

Transport Equation:

$$q_{m,i}(k_s) = \rho_{m,i}(k_s) \cdot v_{m,i}(k_s) \cdot \lambda_i \quad (2.1)$$

Continuity Equation:

$$\rho_{m,i}(k+1) = \rho_{m,i}(k) + \frac{T}{L_i \cdot \lambda_i} [q_{m,i-1}(k) - q_{m,i}(k) + r_i(k) - s_i(k)] \quad (2.2)$$

Speed Equation:

$$v_{m,i}(k+1) = v_{m,i}(k) + \frac{T}{\tau} \left[V(\rho_{m,i}(k)) - v_{m,i}(k) \right] + \frac{T}{L_i} v_{m,i}(k) \cdot [v_{m,i-1}(k) - v_{m,i}(k)] - \frac{vT[\rho_{m,i+1}(k) - \rho_{m,i}(k)]}{\tau L_i [\rho_{m,i}(k) + \kappa]} \quad (2.3)$$

Fundamental Diagram:

$$V(\rho_{m,i}(k)) = v_{f,m} \cdot \exp \left[-\frac{1}{a_m} \left(\frac{\rho_{m,i}(k)}{\rho_{cr,m}} \right)^{a_m} \right] \quad (2.4)$$

$$Q(\rho_{m,i}(k_s)) = \rho_{m,i}(k_s) \cdot v_{f,m} \cdot \exp \left[-\frac{1}{a_m} \left(\frac{\rho_{m,i}(k)}{\rho_{cr,m}} \right)^{a_m} \right] \quad (2.5)$$

where $r_i(k)$, $s_i(k)$ are the on-ramp inflow and off-ramp outflow, respectively; $v_{f,m}$ and ρ_{cr} are the free-flow speed and critical density, respectively; functions V , Q provide a speed and a flow value for the cell i of the stretch m , respectively; $\tau(\tau)$, $v(nue)$, $\kappa(kappa)$ are global parameters given for the whole network. More specifically, τ is a time constant; v is an anticipation constant; and κ is a model parameter. So, the first term of Equation (2.3) express the relaxation time, the second term express the convection between the cells and the third one, the anticipation of the network. Equations (2.1)- (2.4) are only applied to normal stretches inside the network.

If the network consists of several stretches that merge at a node or there are leaving links (on-ramps – off ramps), merging phenomena have to be considered. This can be achieved by adding the following term to speed Equation (2.3):

$$-\frac{\delta T}{L_i \cdot \lambda_i} \cdot \frac{r_1(k) \cdot v_{m,i}(k)}{\rho_{m,i}(k) + \kappa}, \quad (2.6)$$

where δ is a global parameter.

2.4.3 Fundamental Diagram

The fundamental diagram (FD) of traffic flow is a diagram that gives the relationship between the traffic flow and the traffic density in cell i of stretch m . On the previous section, the free flow speed $v_{f,m}$ (*vfree*), the critical density $\rho_{cr,m}$ (*rocrit*), for which the flow at cell i is maximized, and the exponent a_m , are designed for the construction of fundamental diagram (Equations (2.4)-(2.5)) of the considered stretch m . The Equation (2.5) is used to design the FD of cell i of stretch m is an empirical relation.

FD represents the capacity of each cell in terms of vehicle density. Maximum capacity (q_{cap}) of cell i is the region that the traffic density becomes critical (*rocrit*) and traffic flow is maximized. The shape of the fundamental diagram is determined by the parameters $v_{f,m}$, $\rho_{cr,m}$ and a_m (no direct physical significance), which are

specific for each FD. The FD can be presented either by a triangular or either by a parabolic curve. Here, the FD of each cell is described by the following parabolic shaped flow - density diagram. Related studies support that triangular shaped flow - density diagram is an accurate representation of real world events in comparison with parabolic shaped flow - density diagram. Although, in theoretical level, the first type of FD is been used efficiently.

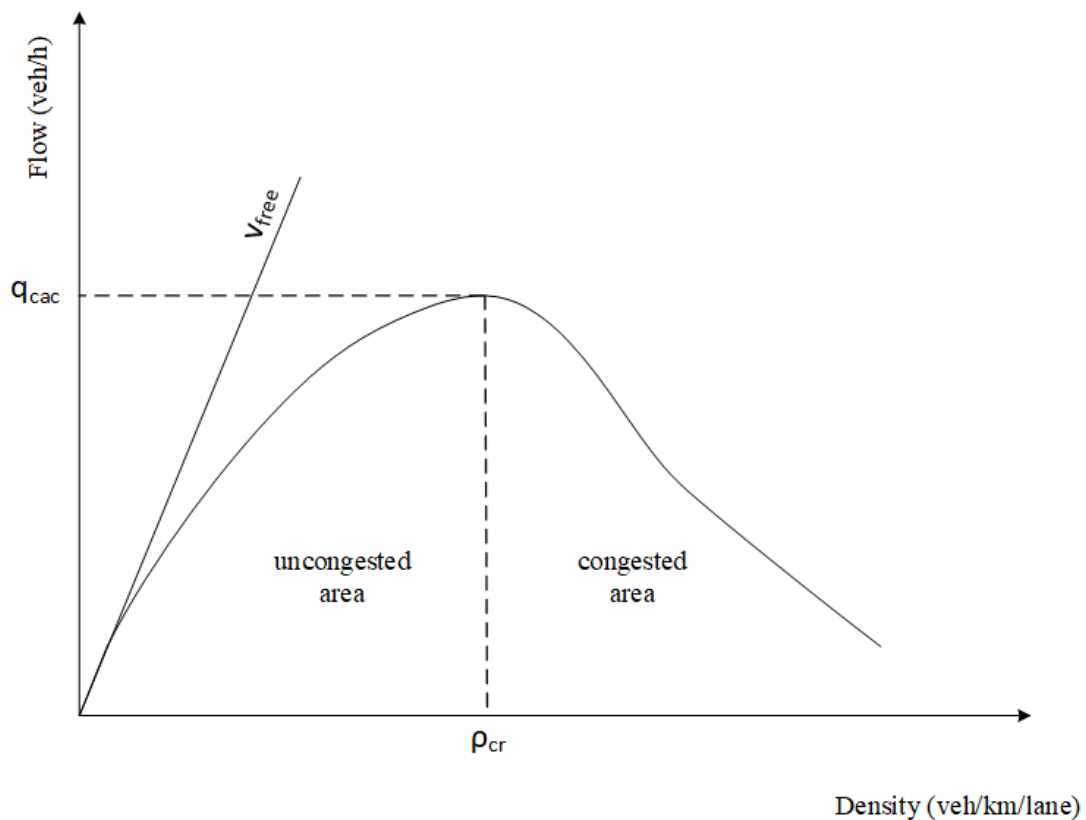


Figure 3: Flow-Density diagram

Each FD consists of two regions. The one represents the uncongested area and the other one the congested area. Congestion appears when the network characterized of maximum capability (q_{cap}). Thus, as it is shown in Figure 3, $v_{f,m}$ (v_{free}) can be found by calculating the slope of the tangent at a point of FD's uncongested area. This

slope indicates the linearized speed that is denoted by v_f (*free*) if the linearization point is zero or by $v_{lin,i}$ if the linearization point is near the critical density.

The continuity Equation (2.3) is a dynamical equation that expresses the conservation of vehicles within the network. Taking into consideration the Generalized Cell Transmission Model (CTM), the uncongested area of the FD, the linearization at a point of the FD and the absence of on-ramps and off-ramps at the region of linearization, the continuity equation is

$$\rho_{m,i}(k+1) = \rho_{m,i}(k) + \frac{T}{L_i \cdot \lambda_i} [v_{lin,i-1} \rho_{m,i-1}(k) - v_{lin,i} \rho_{m,i}(k)] \quad (2.7)$$

Thus,

$$\rho_{m,i}(k+1) = \left[1 - \frac{T}{L_i \cdot \lambda_i} v_{lin,i}\right] \rho_{m,i}(k) + \frac{T}{L_i \cdot \lambda_i} v_{lin,i-1} \rho_{m,i-1}(k) \quad (2.8)$$

The Equation (2.2) is similar to the Equation (2.8) with the difference that the second equation depends on the value of the slope of the FD ($v_{lin,i}$) near the critical density. This expression will be useful to explain how LQI regulator is constructed and it is described in the following section.

3. LQI Regulator

3.1 Introduction

The theory of optimal control is concerned with operating a dynamic system at minimum cost. The case where the system dynamics are described by a set of linear differential equations and the cost is described by a quadratic function is called the LQ problem. The solution is provided by the linear quadratic regulator (LQR), a feedback controller, which is an important part of the solution to the LQI (Linear Quadratic Integral) problem. The LQI algorithm reduces the amount of work done by the user to optimize the controller [8], [4]. However, the user still needs to specify the cost function parameters, and compare the results with the specified design values. Thus, the controller construction will be an iterative process in which the user evaluates the "optimal" controllers produced through simulation and then adjusts the parameters to produce a controller more consistent with design values. The LQR, and in specific the LQI algorithm, is essentially an automated way of finding an appropriate state-feedback controller.

3.2 LQI Formulation

The kinematic wave Lighthill-Whitham-Richards (LWR) model is a scalar nonlinear conservation law of hyperbolic type and turns out to be one of the simplest nonlinear conservation laws. LWR type models represent a valuable tool for the study of traffic behavior because of their simplicity, efficiency under congesting conditions. In order to derive the LQI regulator for local ramp metering (single on-ramp control), the system is described by a set of nonlinear differential equations (3.1):

$$\rho(k + 1) = F(\rho(k), r(k)), \quad (3.1)$$

where F is a nonlinear function reflecting the discretized LWR model [8], $\boldsymbol{\rho}(k) \in \mathfrak{R}^n$ denotes the densities corresponding in freeway sections between the on-ramp and the bottleneck and $r(k) \in \mathfrak{R}$ denotes the on-ramp flow, at time step k . Linearization of this system around the steady-state $(\boldsymbol{\rho}^d, r^d)$ yields to the following equation:

$$\Delta\boldsymbol{\rho}(k+1) = \mathbf{A}\Delta\boldsymbol{\rho}(k) + \mathbf{B}\Delta r(k), \quad (3.2)$$

where $\Delta\boldsymbol{\rho}(k) = \boldsymbol{\rho}(k) - \boldsymbol{\rho}^d$ and $\Delta r(k) = r(k) - r^d$ denote the linearized state vector and control input, respectively. $\mathbf{A} \in \mathfrak{R}^{n \times n}$ and $\mathbf{B} \in \mathfrak{R}^{n \times 1}$ are the state and input matrices.

In order to include integral parts into the state regulator, we consider now the state Equation (3.2) augmented by the use of

$$y(k+1) = y(k) + \mathbf{H}\Delta\boldsymbol{\rho}(k), \quad (3.3)$$

where $y \in \mathfrak{R}$ and $\mathbf{H} \in \mathfrak{R}^{1 \times n}$ is a horizontal vector, which has a one at the n^{th} component (so that the bottleneck density is integrated in (3.3)) and 0's elsewhere. For deriving the LQI control, the control goal is to minimize the quadratic criterion:

$$J = \frac{1}{2} \sum_{k=0}^{\infty} [\|\Delta\boldsymbol{\rho}(k)\|_{\tilde{\mathbf{Q}}}^2 + \|\Delta r(k)\|_{\tilde{\mathbf{R}}}^2 + \|y(k)\|_{\tilde{\mathbf{S}}}^2], \quad (3.4)$$

where $\mathbf{Q} \in \mathfrak{R}^{n \times n}$ is a symmetric positive definite weighting matrix and $R, S \in \mathfrak{R}$ correspond to positive constants. Considering the Equations (3.3) and (3.4) the following augmented matrices for LQI control are obtained:

$$\tilde{\mathbf{A}} = \begin{bmatrix} \mathbf{A} & \mathbf{0} \\ \mathbf{H} & 1 \end{bmatrix}, \quad \tilde{\mathbf{B}} = \begin{bmatrix} \mathbf{B} \\ 0 \end{bmatrix}, \quad \tilde{\mathbf{Q}} = \begin{bmatrix} \mathbf{Q} & \mathbf{0} \\ \mathbf{0} & S \end{bmatrix}, \quad \tilde{R} = R, \quad (3.5)$$

leading to the following time-invariant solution:

$$\Delta r(k) = -\tilde{\mathbf{K}} \begin{bmatrix} \Delta \boldsymbol{\rho}(k) \\ y(k) \end{bmatrix}, \quad (3.6)$$

where $\tilde{\mathbf{K}}$ is the gain matrix depending on the problem matrices $\tilde{\mathbf{A}}, \tilde{\mathbf{B}}, \tilde{\mathbf{Q}}, \tilde{\mathbf{R}}$. Matrix $\tilde{\mathbf{K}}$ is a horizontal vector that may be calculated by the backward integration of the augmented Riccati matrix $\tilde{\mathbf{P}}(k)$ starting from any terminal condition $\tilde{\mathbf{P}}(K) \geq 0$ until convergence towards a unique stationary value $\tilde{\mathbf{P}} \geq 0$ is obtained. The gain matrix $\tilde{\mathbf{K}}$ is specified by solving the following system equation:

$$\tilde{\mathbf{P}} = \tilde{\mathbf{A}}^T \mathbf{P} \tilde{\mathbf{A}} + \tilde{\mathbf{Q}} - \tilde{\mathbf{K}}^T \tilde{\mathbf{B}}^T \mathbf{P} \tilde{\mathbf{A}} \quad (3.7)$$

$$\tilde{\mathbf{K}} = (\tilde{\mathbf{B}}^T \mathbf{P} \tilde{\mathbf{B}} + \tilde{\mathbf{R}})^{-1} \tilde{\mathbf{B}}^T \mathbf{P} \tilde{\mathbf{A}}, \quad (3.8)$$

where Equation (3.7) denotes the algebraic Riccati equation. Decomposing $\tilde{\mathbf{K}} = [\mathbf{K}_x \quad \mathbf{K}_y]$, we obtain from (3.8):

$$\Delta r(k) = -\mathbf{K}_x \Delta \boldsymbol{\rho}(k) - \mathbf{K}_y y(k) \quad (3.9)$$

Considering Equation (3.3), the Equation (3.9) is obtained

$$\Delta r(k) = -\mathbf{K}_x \Delta \boldsymbol{\rho}(k) - \mathbf{K}_y y(k+1) + \mathbf{K}_y \mathbf{H} \Delta \boldsymbol{\rho}(k) \quad (3.10)$$

After some algebra by subtracting above equation at $k-1$ from the same equation at k , and considering the Equation (3.3), we get

$$r(k) = r(k-1) - (\mathbf{K}_x - \mathbf{K}_y \mathbf{H}) [\boldsymbol{\rho}(k) - \boldsymbol{\rho}(k-1)] + \mathbf{K}_y \mathbf{H} \Delta \boldsymbol{\rho}(k), \quad (3.11)$$

thus getting the LQI feedback control law:

$$r(k) = r(k-1) - (\mathbf{K}_x - K_y \mathbf{H})[\boldsymbol{\rho}(k) - \boldsymbol{\rho}(k-1)] + K_y \mathbf{H}[\rho_n^d - \rho_n(k)], \quad (3.12)$$

where $\rho_n(k)$ and ρ_n^d indicate the bottleneck's state and desired state, respectively.

Setting now:

$$\mathbf{K}_P = \mathbf{K}_x - K_y \mathbf{H}$$

$$K_I = K_y \mathbf{H}$$

The final LQI controller is obtained:

$$r(k) = r(k-1) - \mathbf{K}_P[\boldsymbol{\rho}(k) - \boldsymbol{\rho}(k-1)] + K_I[\rho_n^d - \rho_n(k)] \quad (3.13)$$

Similar to the application of PI-ALINEA, in order to avoid wind-up-effects, the feedback LQI regulator (3.13) is truncated if it exceeds a range $[r^{min}, R^{max}(k)]$, where $R^{max}(k) = \min(r^{min}, r^{max}(k-1) + 400)$, r^{min} and r^{max} are the minimum and maximum admissible on-ramp flow, respectively, $r^{min}(k-1)$ is the measured ramp inflow during the last control time interval with 400 being an empirical value.

$$r(k_c) = \max(r^{min}, \min(R^{max}(k_c), r(k_c-1) - \mathbf{K}_P[\boldsymbol{\rho}(k_c) - \boldsymbol{\rho}(k_c-1)] + K_I[\rho_n^d - \rho_n(k_c)]) \quad (3.14)$$

4. Local Ramp Metering using LQI

4.1 Simulation model and simulation set-up

METANET traffic flow model that described before, has been used to simulation investigations. Five freeway stretches are considered in the following section. The critical density for METANET equations is defined as $\rho_{cr} = 31.4$ veh/km/lane for each stretch; the parameter $a = 2$; $v_{f1} = 105$ km/h about non-bottleneck cells; $v_{f2} = 79$ km/h about bottleneck cells; $\tau(\tau\text{au}) = 20/3600$ h; $v(\text{nue}) = 35$ km²/h, $\kappa(\text{kappa}) = 13$ veh/km/h. For LQI formulation r^{min} and r^{max} are set equal to 300 and 2000 veh/h, respectively [9], [10].

4.1.1 Network Description

In this thesis, for modelling and simulation, a freeway network of $N = 32$ cells, is considered (Figure 4-Figure 8), for each of five bottleneck cases have been tested. The network has a main entrance (cell 1), one exit (cell 32) and a single on-ramp located at the upstream boundary of the ninth (9th) cell, which is 2 km downstream from the network entrance. The length of each cell is $L_i = 0.25$ km. Each cell has $l_i = 3$ lanes. Thus, the total length of the freeway is 8 km. The length of each bottleneck is 1 km (4 cells) and it is assumed to be present in different locations downstream of the on-ramp for the different control scenarios (see the grey areas in Figure 4-Figure 8).

Five bottleneck cases are described here. In the first case, the bottleneck is located at cell 10, near the on-ramp at the 9th cell (Figure 3). Thus, each of the five cases have a 1 km-long bottleneck at locations 0.25 km, 1.5 km, 2.75 km, 4 km and 5 km, respectively, downstream of the on-ramp (Figure 4-Figure 8).

The linearized (considered) system extends from the on-ramp location (cell 9) to the first cell of the bottleneck section (see the areas indicated by circles in Figure 4-Figure 8). These cells N' indicate the number of considered cells of the network.

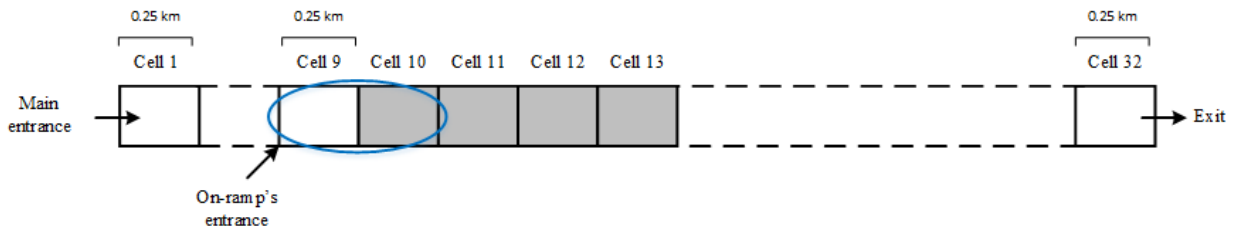


Figure 4: Bottleneck case 1

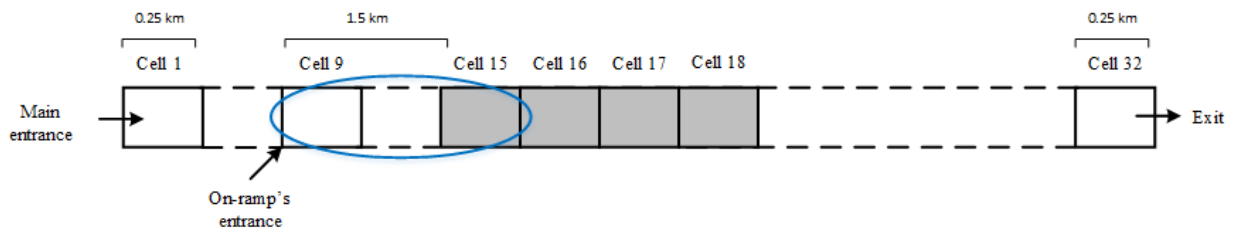


Figure 5: Bottleneck case 2

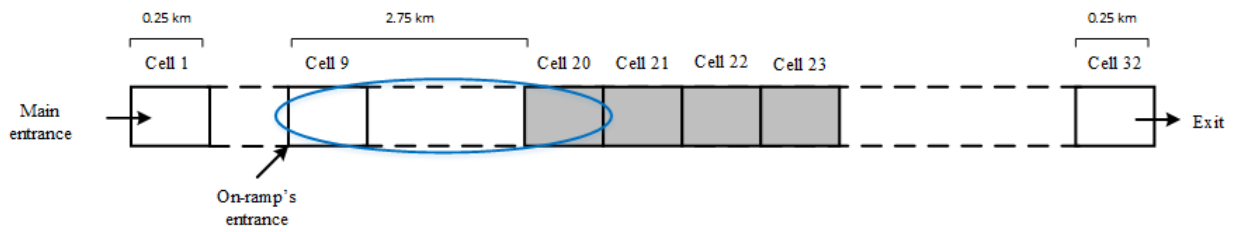


Figure 6: Bottleneck case 3

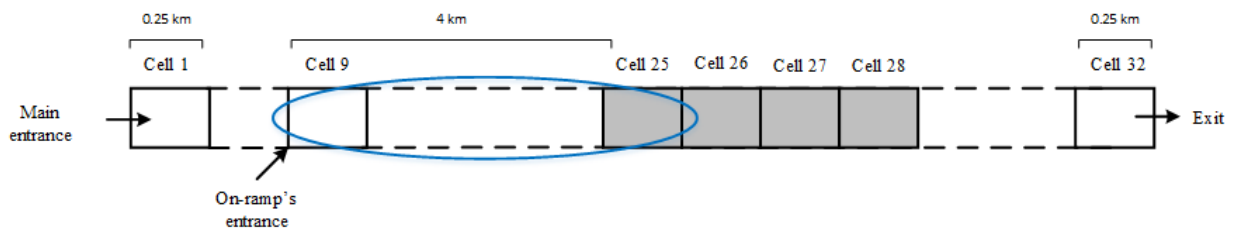


Figure 7: Bottleneck case 4

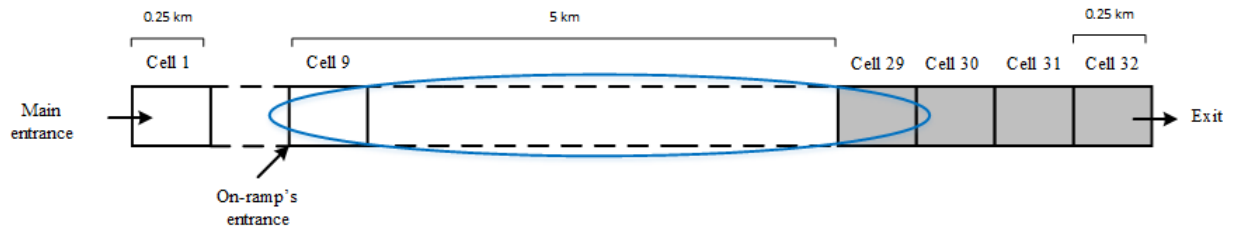


Figure 8: Bottleneck case 5

4.1.2 Fundamental Diagram and Demand scenarios

A bottleneck section differs from a non-bottleneck section in traffic flow characteristics. More specifically, the fundamental diagram “FD for non-bottlenecks cells” is included to the simulation model to emulate each non-bottleneck cell, whereas “FD for bottlenecks cells” is considered for each bottleneck cell (Figure 9). Bottleneck cells are characterized by FDs with lower capacity compared to non-bottleneck cells.

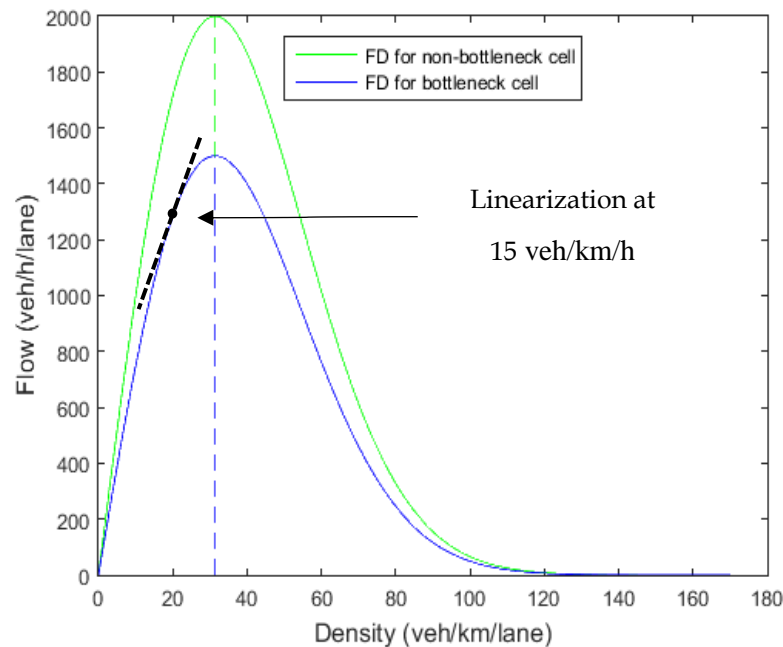


Figure 9: Fundamental diagrams considered

Thus, $q_{cap1} = 2000$ veh/h/lane and $q_{cap2} = 1500$ veh/h/lane about non-bottleneck and bottleneck cells, respectively, are the maximum capacities while density is critical $\rho_{cr} = 31.4$ veh/km/lane. As shown in Figure 9, two FD's have the same critical density, but different free speeds (linearized speeds) and capacities. The slope of the tangent of FD diagram (uncongested area) at point 15 veh/km/h, near the critical density, denotes the linearized speed at this point.

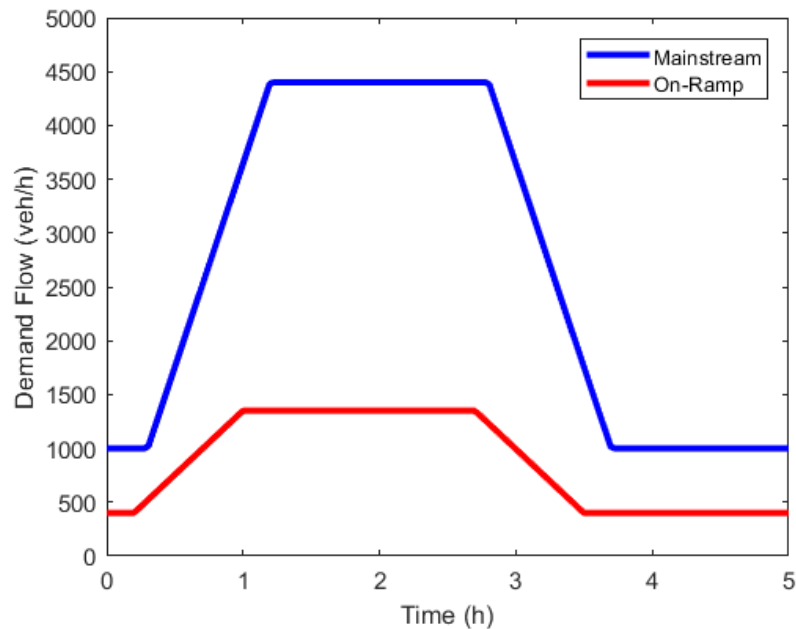


Figure 10: Utilized mainstream and on-ramp demand scenarios

The trapezoidal demand scenarios shown in Figure 10 are used in the simulation investigations over a time horizon 4 h. This figure presents the considered entrance and on-ramp demand scenarios. The trapezoidal demand of the mainstream entrance reaches the value of 4400 veh/h and the demand of the on-ramp reaches the value of 1350 veh/h.

4.2 Control set-up

The simulation time step T and control time step T' are 5 sec and 30 sec, respectively. Measurements of flow and density for each cell i of each considered freeway stretch, are extracted from the simulator every $T = 5$ sec. Then, the average of these measurements is fed to the regulator (Equation (3.14)) of the LQI every $T' = 30$ sec.

Therefore, the dimension of density ρ and the dimensions of corresponding matrices A, B, Q, H, R, S considered in Section for LQI Formulation depends on the bottleneck location (see Figure 4: Bottleneck case1Figure 8: Bottleneck case 5). The number of considered cells, indicating with circles in Figure 4: Bottleneck case1Figure 8: Bottleneck case 5, is expressed by the symbol N' . In particular, according to the Equation (2.8), the matrices A and B are formulated as follows:

$$A_{N' \times N'} = \begin{bmatrix} 1 - \frac{T}{L_1 \lambda_1} v_{lin,1} & 0 & \cdots & \cdots & \cdots & 0 \\ \frac{T}{L_2 \lambda_2} v_{lin,1} & 1 - \frac{T}{L_2 \lambda_2} v_{lin,2} & 0 & \vdots & \vdots & \vdots \\ 0 & \frac{T}{L_3 \lambda_3} v_{lin,2} & \ddots & \vdots & \vdots & \vdots \\ \vdots & 0 & \vdots & \ddots & 0 & \vdots \\ \vdots & \vdots & 0 & \vdots & 1 - \frac{T}{L_{N'-1} \lambda_{N'-1}} v_{lin,N'-1} & 0 \\ 0 & \cdots & \cdots & 0 & \frac{T}{L_{N'} \lambda_{N'}} v_{lin,N'-1} & 1 - \frac{T}{L_{N'} \lambda_{N'}} v_{lin,N'} \end{bmatrix}$$

$$B_{N' \times 1} = \begin{bmatrix} \frac{T}{L_1 \lambda_1} \\ 0 \\ \vdots \\ \vdots \\ 0 \\ 0 \\ 0 \end{bmatrix}$$

The linearized speed at point 15 veh/km/h for non-bottleneck cells is set equal to $v_{lin,1} = 72$ km/h and for bottleneck cells equal to $v_{lin,2} = 54$ km/h. The matrix H is formulated as following (taking into consideration the single on-ramp):

$$H_{N' \times 1} = [0 \quad 0 \quad \dots \quad \dots \quad \dots \quad \dots \quad \dots \quad 0 \quad 1]$$

For deriving the gain matrices K_p, K_I an appropriate selection of the weighting matrices Q, R, S should be performed. After extensive simulation tests, in this study these matrices are:

$$Q_{N' \times N'} = \begin{bmatrix} \frac{10^4}{N'} & \dots & \dots & \dots & \dots & \dots \\ \vdots & \frac{10^4}{N'} & \vdots & \vdots & \vdots & \vdots \\ \vdots & \vdots & \ddots & \vdots & \vdots & \vdots \\ \vdots & \vdots & \vdots & \ddots & \vdots & \vdots \\ \vdots & \vdots & \vdots & \vdots & \frac{10^4}{N'} & \vdots \\ \dots & \dots & \dots & \dots & \dots & \frac{10^6}{N'} \end{bmatrix}$$

$$R_{1 \times 1} = 1$$

$$S_{1 \times 1} = 10^4$$

For each of these network scenarios described before, no control and control results under the LQI and PI-ALINEA, are presented.

5. *Simulation Investigations*

Here, the simulation investigation results are presented. Five typical scenarios of bottlenecks are considered in this thesis (Bottleneck case 1, Bottleneck case 2, Bottleneck case 3, Bottleneck case 4, Bottleneck case 5) and two configurations of ramp metering controllers are considered for each scenario (ramp metering with LQI, ramp metering with PI-ALINEA). For each scenario there is a bottleneck of 1 km at various locations downstream of the on-ramp. Also, the no control case is presented for each bottleneck case. It is important to note that the set-point used for both regulators is the factual critical density of each bottleneck cell, which is different with the one given as FD parameter, due to METANET model dynamics (see Table 1).

5.1 *Set point selection*

For bottleneck case 1, 2, 3, 4 and 5, the factual density of the first bottleneck cell was found around 42, 41, 39, 39 and 42 veh/km/lane (Table 1), respectively (instead of 31.4 veh/km/lane), used also as set-point for the control application.

Taking into consideration the considered (linearized system) that described before, the dimension of the gain matrices K_p, K_I depend on the bottleneck location. For each bottleneck case, matrices K_p, K_I are formulated as follows (see Table 2):

Table 1: Set-point selection

	Set Point (veh/km/lane)	Stationary Flow (veh/h)
Bottleneck Cases		
	41	5193
1	42	5194
	43	5192
	40	5270
2	41	5269
	42	5267
	38	5279
3	39	5282
	40	5283
	38	5280
4	39	5283
	40	5284
	41	5084
5	42	5084
	43	5082

Table 2: Gain values for each bottleneck case

Bottleneck Cases	1	2	3	4	5
N'	2	7	12	17	21
K _P (km*lane/h)	135	124	111	104	99
	125	153	137	126	119
		177	159	147	139
		194	178	165	157
		204	192	181	173
		208	202	193	186
		146	207	201	196
			210	207	203
			212	211	208
			212	212	211
			212	213	213
			149	214	214
				214	215
				214	215
				214	215
				150	215
					215
				215	
				215	
				151	
K _I (km*lane/h)	61	63	64	64	65

5.2 Simulation Investigations- Bottleneck case 1

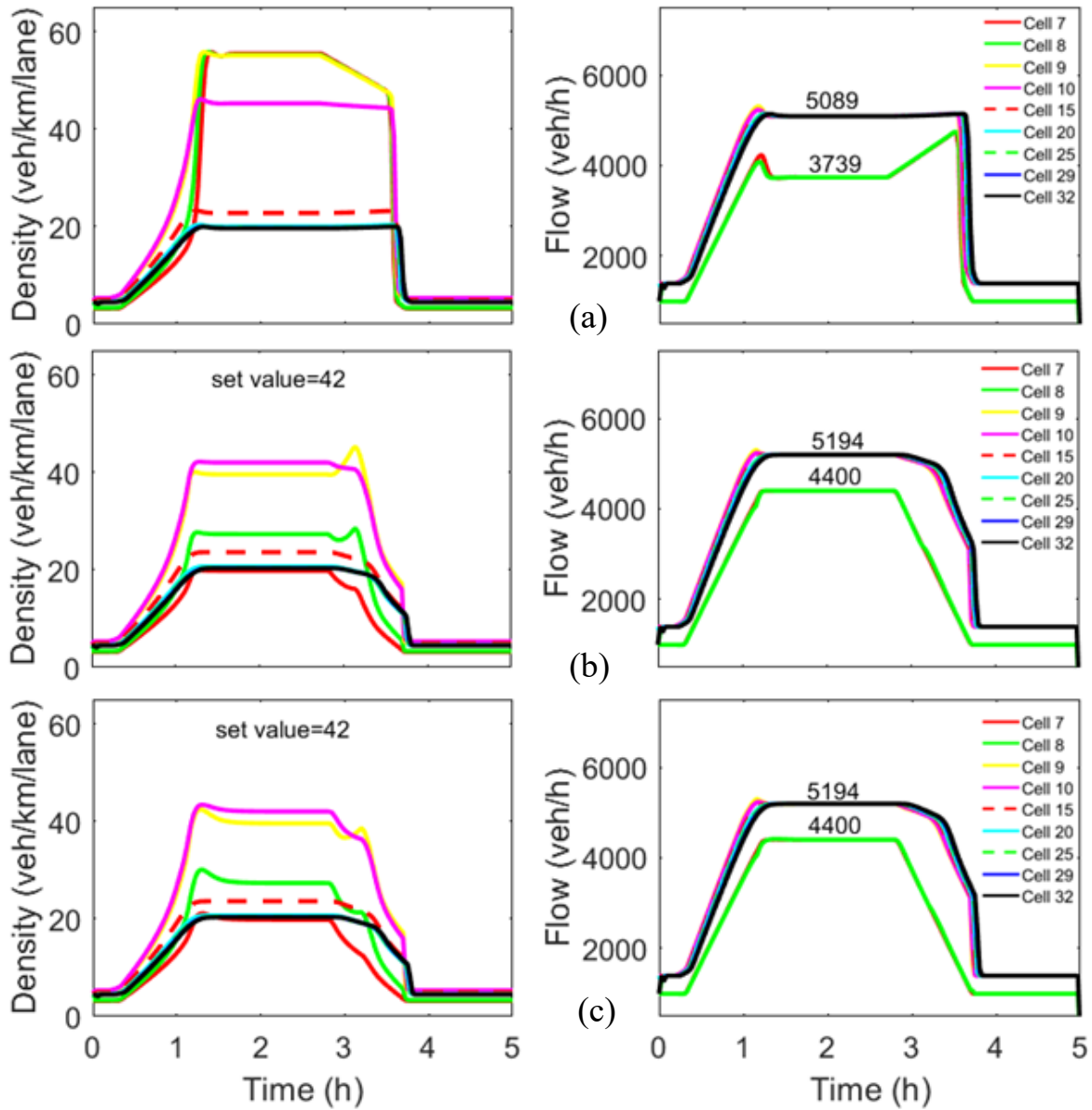


Figure 11: Bottleneck case 1: (a) No control case, (b) control case with LQI, (c) control case with PI-A LINEA

The bottleneck case 1 (see Figure 1) has a bottleneck of 1 km (cell 10 to cell 13) located at cell 10, near the on-ramp's entrance (cell 9). The linearized (considered) system extends from the upstream boundary of cell 9 to the first cell of the bottleneck section (cell 10).

No Control Case: As shown in Figure 11(a), a severe congestion is created in the freeway mainstream resulting accordingly to capacity drop. The total demand (mainstream and on-ramp's demand = 5750 veh/h) entering the merging area during the peak period exceeds considerably the capacity level of cell 9. The density of cell 9 reaches the critical value of 42 veh/km/lane at about $t = 1.3$ h, at which time that the stationary flow of cell 9 reaches the capacity level. As the density continues to increase, congestion initially builds in the bottleneck cell (cell 10) and gradually spills back to the upstream cells. Due to the uncontrollable on-ramp inflow, the mainstream demand upstream of the on-ramp cannot be efficiently served. Thus, the cells downstream the bottleneck location are not congested. Consequently, the outflow of cell 9 is around to 5089 veh/h.

LQI: For bottleneck case 1 shown in Figure 11(b), the factual critical density and the stationary flow (of three lanes) for the bottleneck cell are found to be around 42 veh/km/lane and 5194 veh/h, respectively. As is shown in Figure 11(b), the density becomes undercritical much earlier than in the no control case. The ramp metering action leads to a corresponding reduction of the total time spent by all vehicles. The density of cell 10 is kept exactly at the set value, whereas the capacity level of the bottleneck section is achieved, and the mainstream demand is well served.

PI-ALINEA: For bottleneck case 1 shown in Figure 11(c), the ramp metering results by PI-ALINEA are so satisfactory as the results by LQI. As in LQI case, the factual density and the stationary flow for cell 10 are found equal to 42 veh/km/lane and 5194 veh/h, respectively. For PI-ALINEA's action, K_p, K_I gains as set equal to 100, 4 km*lane/h, respectively.

5.3 Simulation Investigations- Bottleneck case 2

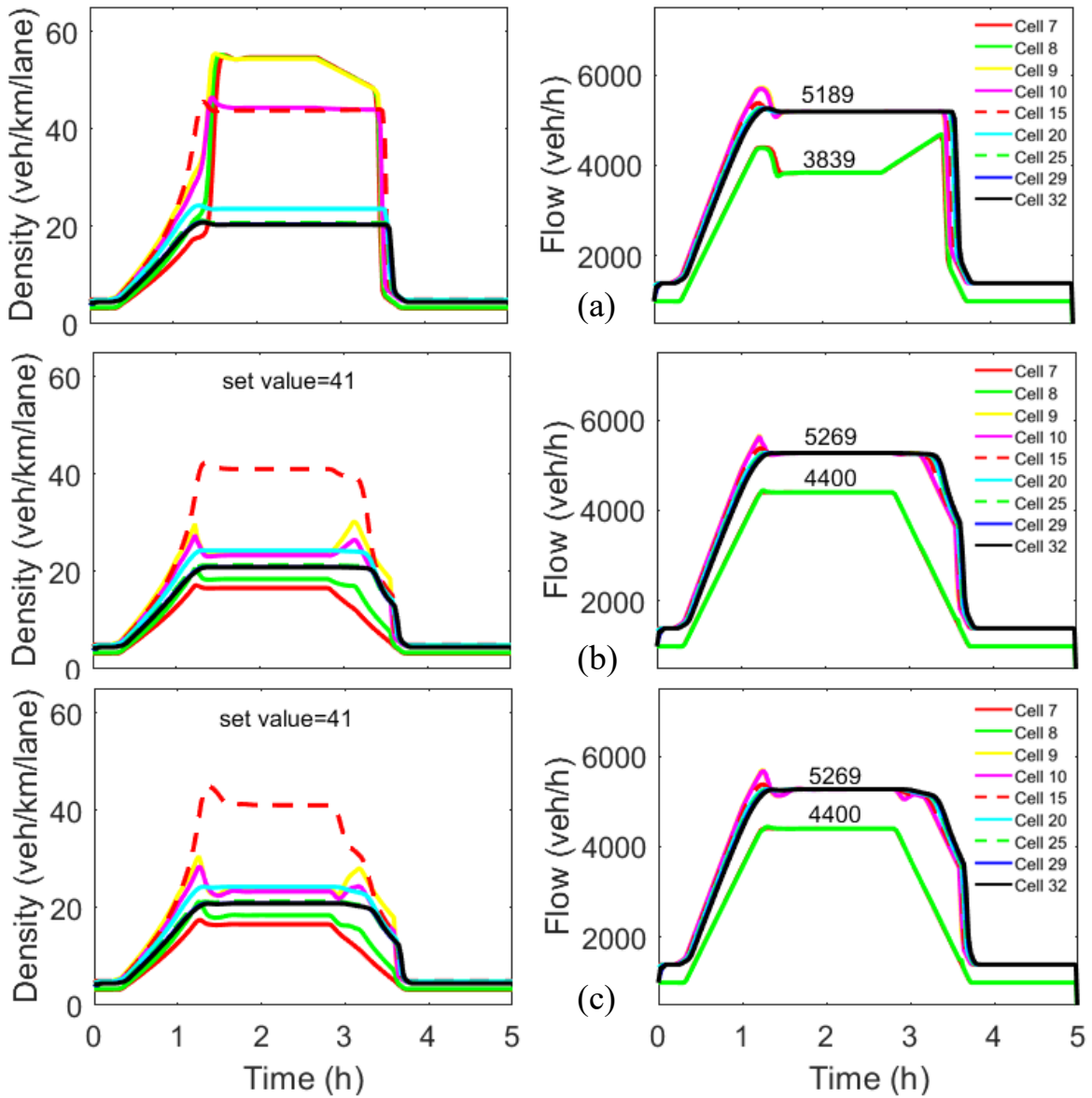


Figure 12: Bottleneck case 2: (a) No control case, (b) control case with LQI, (c) control case with PI-ALINEA

The bottleneck case 2 (see Figure 5) has a bottleneck of 1 km (cell 15 to cell 18) located at cell 15, downstream the on-ramp's entrance (cell 9). The linearized (considered) system extends from the upstream boundary of cell 9 to the first cell of the bottleneck section (cell 15).

No Control Case: As shown in Figure 12(a), a severe congestion is created in the freeway mainstream resulting accordingly to capacity drop. The total demand (mainstream and on-ramp's demand = 5750 veh/h) entering the merging area during the peak period exceeds considerably the capacity level of cell 9. The density of cell 9 reaches the critical value of 41 veh/km/lane at about $t = 1.3$ h, at which time the stationary flow of cell 9 reaches the capacity level. As the density continues to increase, congestion initially builds in the bottleneck cell (cell 15) and gradually spills back to the upstream cells. Due to the uncontrollable on-ramp inflow, the mainstream demand upstream of the on-ramp cannot be efficiently served. Thus, the cells downstream the bottleneck location are not congested. Consequently, the outflow of cell 9 is around to 5189 veh/h.

LQI: For bottleneck case 2 shown in Figure 12(b), the factual critical density and the stationary flow (of three lanes) for the bottleneck cell are found to be around 41 veh/km/lane and 5269 veh/h, respectively. The ramp metering action leads to a corresponding reduction of the total time spent by all vehicles. The density of cell 15 is kept exactly at the set value, whereas the capacity level of the bottleneck section is achieved, and the mainstream demand is well served.

PI-ALINEA: For bottleneck case 2 shown in Figure 12(c), the ramp metering results by PI-ALINEA are similar to the results by LQI. As in LQI case, the factual density and the stationary flow for cell 15 are found equal to 41 veh/km/lane and 5269 veh/h, respectively. For PI-ALINEA's action, K_P, K_I gains as set equal to 70, 2 km*lane/h, respectively.

5.4 Simulation Investigations- Bottleneck case 3

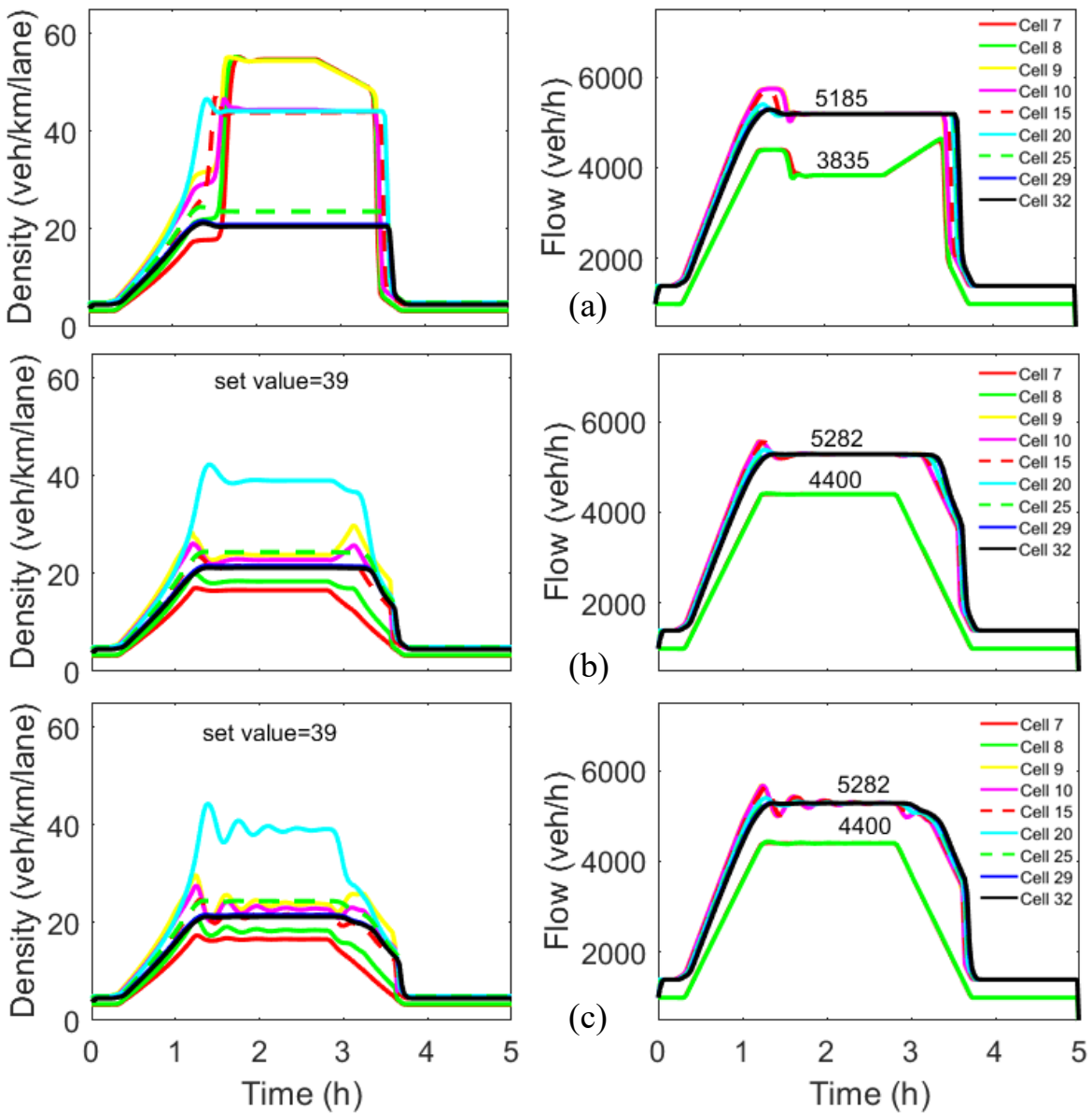


Figure 13: Bottleneck case 3: (a) No control case, (b) control case with LQI, (c) control case with PI-ALINEA

The bottleneck case 3 (see Figure 6) has a bottleneck of 1 km (cell 20 to cell 23) located at cell 20, downstream the on-ramp's entrance (cell 9). The linearized (considered) system extends from the upstream boundary of cell 9 to the first cell of the bottleneck section (cell 20).

No Control Case: As shown in Figure 13(a), a severe congestion is created in the freeway mainstream resulting accordingly to capacity drop. The density of cell 9 reaches the critical value of 39 veh/km/lane at about $t = 1.3$ h, at which time the stationary flow of cell 9 reaches the capacity level. As the density continues to increase, congestion initially builds in the bottleneck cell (cell 20) and gradually spills back to the upstream cells. Due to the uncontrollable on-ramp inflow, the mainstream demand upstream of the on-ramp cannot be efficiently served. Thus, the cells downstream the bottleneck location are not congested. Consequently, the outflow of cell 9 is around to 5185 veh/h.

LQI: For bottleneck case 3 shown in Figure 13(b), the factual critical density and the stationary flow (of three lanes) for the bottleneck cell are found to be around 39 veh/km/lane and 5282 veh/h, respectively. The ramp metering action leads to a corresponding reduction of the total time spent by all vehicles. The density of cell 20 is kept exactly at the set value, whereas the capacity level of the bottleneck section is achieved, and the mainstream demand is well served.

PI-ALINEA: For bottleneck case 3 shown in Figure 13(c), the factual density and the stationary flow for cell 20 are found equal to 39 veh/km/lane and 5282 veh/h, respectively. The resulting density and flow of cell 20 and of the further downstream cells are lightly oscillating around the set value. For PI-ALINEA's action, K_p , K_I gains are set equal to 60, 1 km*lane/h, respectively.

5.5 Simulation Investigations- Bottleneck case 4

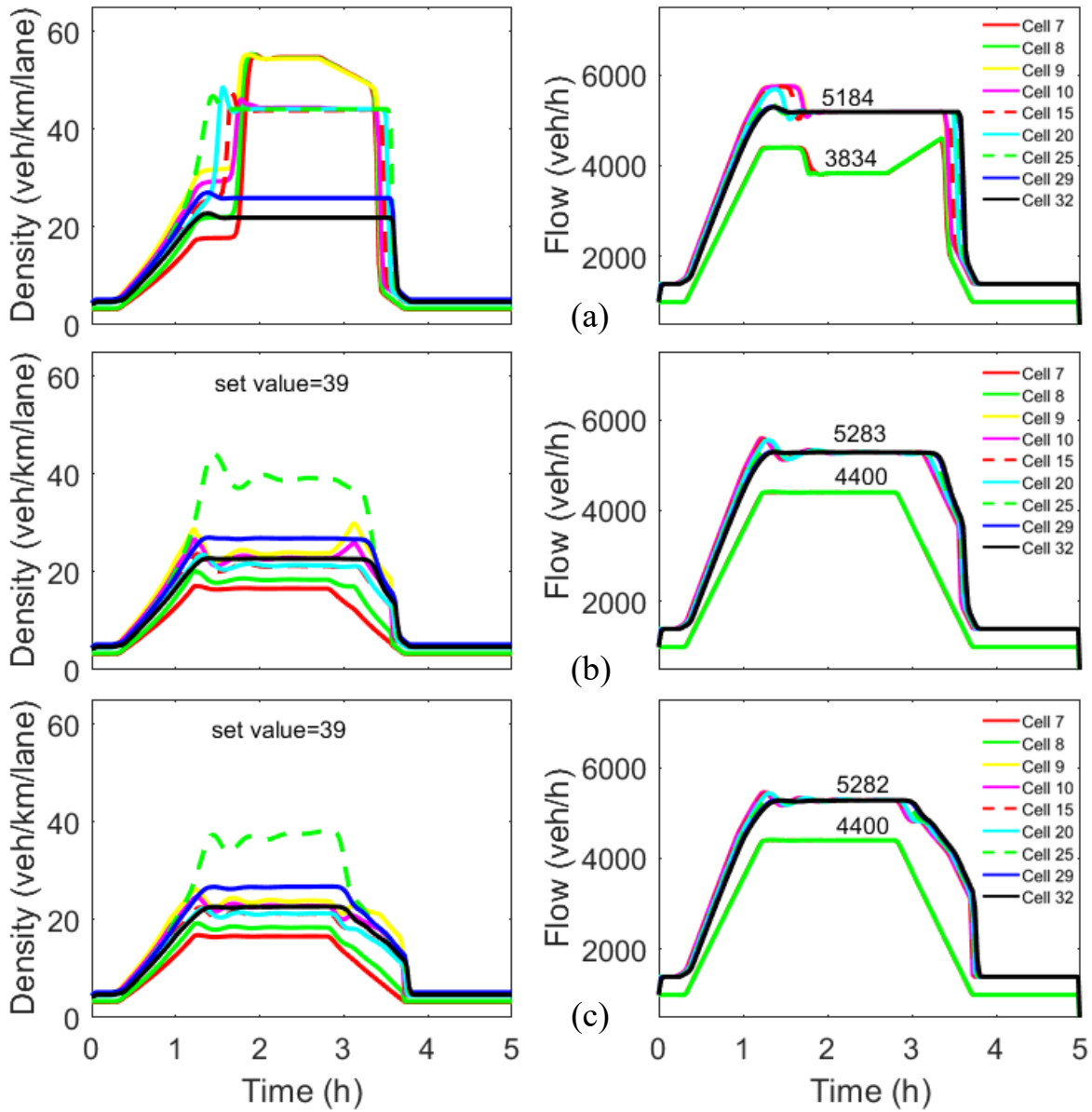


Figure 14: Bottleneck case 4: (a) No control case, (b) control case with LQI, (c) control case with PI-ALINEA

The bottleneck case 4 (see Figure 7) has a bottleneck of 1 km (cell 25 to cell 28) located at cell 25, downstream the on-ramp's entrance (cell 9). The linearized (considered) system extends from the upstream boundary of cell 9 to the first cell of the bottleneck section (cell 25).

No Control Case: As shown in Figure 14(a), a severe congestion is created in the freeway mainstream resulting accordingly to capacity drop. The density of cell 9 reaches the critical value of 39 veh/km/lane at about $t = 1.3$ h, at which time the stationary flow of cell 9 reaches the capacity level. As the density continues to increase, congestion initially builds in the bottleneck cell (cell 25) and gradually spills back to the upstream cells. Due to the uncontrollable on-ramp inflow, the mainstream demand upstream of the on-ramp cannot be efficiently served. Thus, the cells downstream the bottleneck location are not congested. Consequently, the outflow of cell 9 is around to 5184 veh/h.

LQI: For bottleneck case 4 shown in Figure 14(b), the factual critical density and the stationary flow (of three lanes) for the bottleneck cell are found to be around 39 veh/km/lane and 5282 veh/h, respectively. As is shown in Figure 14(b), the ramp metering action leads to a corresponding reduction of the total time spent by all vehicles. The density of cell 25 is lightly oscillating around the set value, whereas the capacity level of the bottleneck section is achieved, and the mainstream demand is well served.

PI-ALINEA: For bottleneck case 4 shown in Figure 14(c), the factual density and the stationary flow for cell 25 are found equal to 39 veh/km/lane and 5282 veh/h, respectively. The resulting density and flow of cell 25 and of the further downstream cells are lightly oscillating around the set value. For PI-ALINEA's action, K_p, K_I gains are set equal to 40, 0.4 km*lane/h, respectively.

5.6 Simulation Investigations- Bottleneck case 5

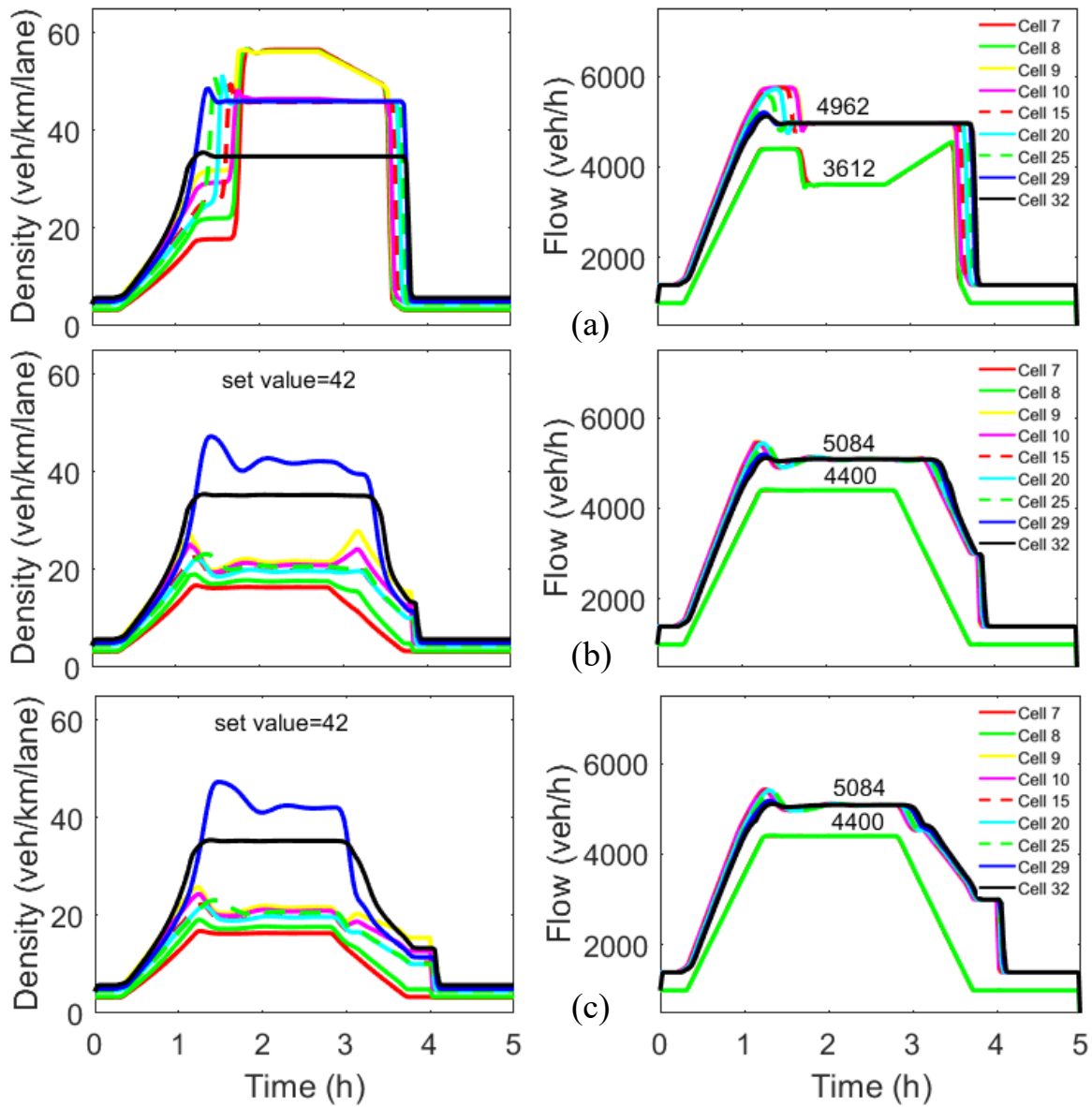


Figure 15: Bottleneck case 5 : (a) No control case, (b) control case with LQI, (c) control case with PI-ALINEA

The bottleneck case 5 (see Figure 8) has a bottleneck of 1 km (cell 29 to cell 32) located at cell 29, downstream the on-ramp's entrance (cell 9). The linearized (considered) system extends from the upstream boundary of cell 9 to the first cell of the bottleneck section (cell 29).

No Control Case: As shown in Figure 15(a), a severe congestion is created in the freeway mainstream resulting accordingly to capacity drop. The density of cell 9 reaches the critical value of 42 veh/km/lane at about $t = 1.3$ h, at which time the stationary flow of cell 9 reaches the capacity level. As the density continues to increase, congestion initially builds in the bottleneck cell (cell 29) and gradually spills back to the upstream cells. Due to the uncontrollable on-ramp inflow, the mainstream demand upstream of the on-ramp cannot be efficiently served. Thus, the cells downstream the bottleneck location are not congested. Consequently, the outflow of cell 9 is around to 4962 veh/h.

LQI: For bottleneck case 5 shown in Figure 15(b), the factual critical density and the stationary flow (of three lanes) for the bottleneck cell are found to be around 42 veh/km/lane and 5084 veh/h, respectively. The ramp metering action leads to a corresponding reduction of the total time spent by all vehicles. The density of cell 29 is lightly oscillating around the set value, whereas the capacity level of the bottleneck section is achieved, and the mainstream demand is well served.

PI-ALINEA: For bottleneck case 5 shown in Figure 15(c), the factual density and the stationary flow for cell 29 are found equal to 42 veh/km/lane and 5084 veh/h, respectively. The resulting density and flow of cell 29 and of the further downstream cells are lightly oscillating around the set value. For PI-ALINEA's action, K_p , K_I gains as set equal to 30, 0.3 km*lane/h, respectively.

The comments on the simulation investigations described before can be summarized for all bottleneck cases:

- *No control case*: In all cases, a congestion is created in the freeway mainstream resulting accordingly to capacity drop. The congestion initially builds in the bottleneck cell and gradually spills back to the upstream cells.
- *RM case*: As simulation tests demonstrate, the performance of LQI and PI-ALINEA (using the gains that proposed) is pretty much the same. Both regulators succeed to avoid mainstream congestion and to achieve a higher throughput. In Table 3, the improvement of the stationary flow is calculated. However, when the bottleneck is moved further downstream (beyond 2 km, including bottleneck cases 3, 4, 5 presented herein), the control task becomes increasingly difficult. Using the same gains for PI-ALINEA leads to aggressive and oscillatory behavior. Thus, as it is described previous, in order to obtain satisfactory performance for PI-ALINEA the gains must change for every different bottleneck case by selecting more and more conservative gains as the bottleneck moves further downstream.

Table 3: Improvement of stationary flow

Bottleneck Cases	Stationary Flow (veh/h)		Improvement (%)
	No control	LQI/PI-ALINEA	
1	5089	5194	2.06%
2	5189	5269	1.54%
3	5185	5282	1.87%
4	5184	5283	1.91%
5	4962	5084	2.46%

5.7 Constant Gains

Taking into consideration the considered (linearized system) and the dimension of the gain matrices by applying LQI (see Table 2), K_p and K_I obtained using weights that lead to smooth and efficient control performance. Although, after extensive simulations, similar performance can be obtained using constant gains K_p and K_I , which are close to the optimal solution. The results presented before are the same in case of using constant values for gains. All the simulation tests for the different bottlenecks have been derived using $K_{p,i} = 200 \text{ km} \cdot \text{lane} / \text{h}$ (where $i = 1, \dots, N'$) and $K_I = 60 \text{ km} \cdot \text{lane} / \text{h}$. Thus, LQI seems to be a robust regulator, because of the low sensitivity in gain selection.

5.8 Control Decision

In Figure 16, the behaviour of control decision is presented for bottleneck cases 1, 2, 3, 4 and 5, using the LQI regulator. According to the on ramp's demand, the control decision seems to be efficient. For bottleneck cases 1, 2, 3, the trajectories of the control decision is smoother than for bottleneck cases 4 and 5 (bottleneck cases downstream the 2 km).

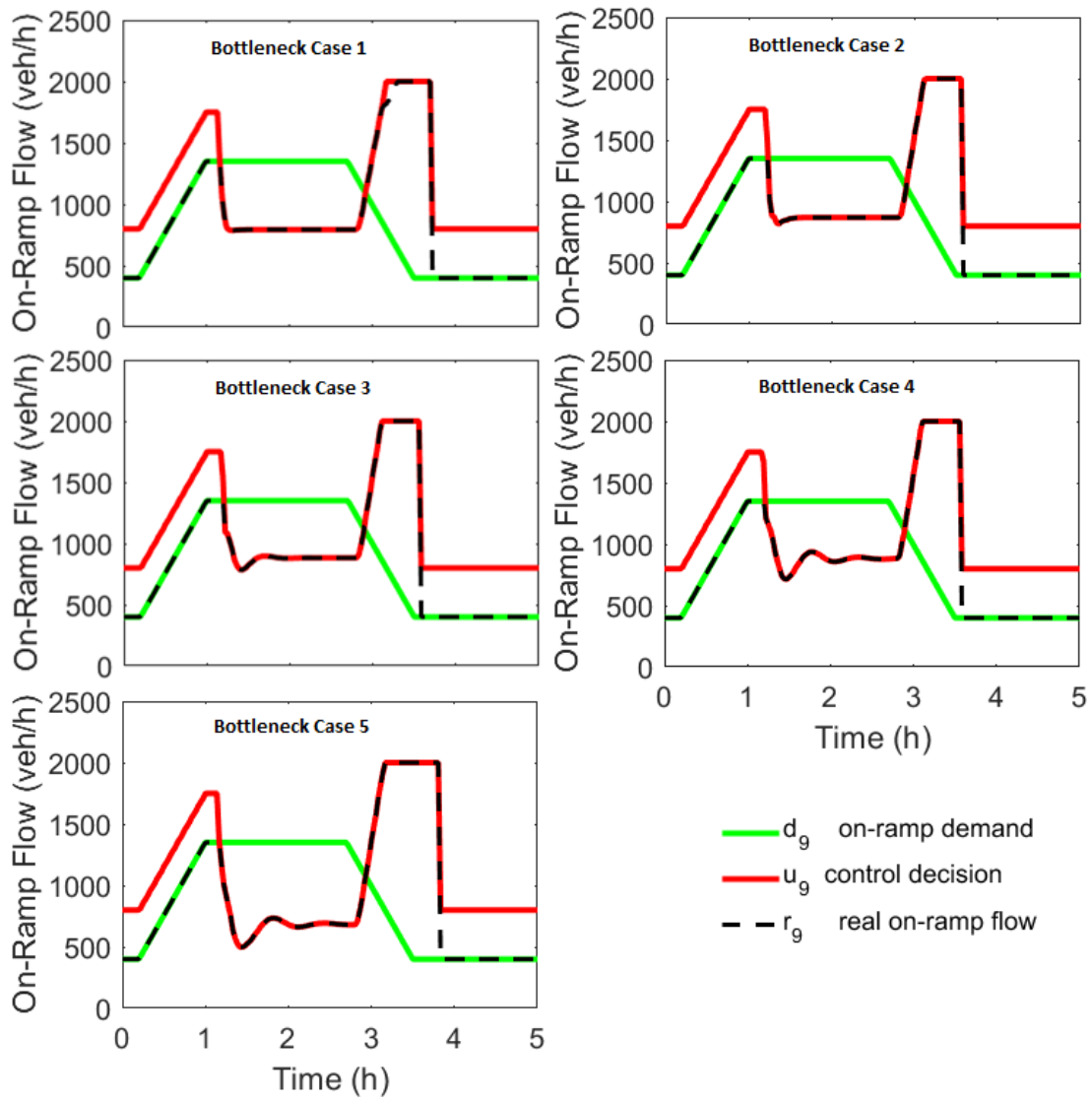


Figure 16: Control decision for each bottleneck case

6. Conclusion and Future Work

The objective of this diploma was to develop and investigate the performance of a Linear Quadratic Regulator augmented with Integral action (LQI) for the freeway ramp metering control problem in case of far downstream bottlenecks. For this reason, a second order model was employed and examined, in particular METANET model, using measurements from the considered network. Thus, the reported theoretical analysis and simulation studies demonstrate that LQI is very efficient in handling the local ramp metering task in the case of very distant downstream bottlenecks (over the 2 km). PI-ALINEA's performance is similar with LQI's. However, the overall study indicates that LQI is much less sensitive in terms of the gains selection, hence easier to deploy. Also, it's important that LQI can handle cases of very distant downstream bottlenecks by setting static gains to construct the regulator.

Future work will focus on integrating LQI within a random-located bottleneck framework. Some random-located bottleneck cases have been tested in related studies via ALINEA ramp metering strategy [8].

References

- [1] T. B. a. B. D. S. A. Hegyi, "Freeway traffic management and control" 2009.
- [2] R. C. CARLSON, "Mainstream traffic flow control" CHANIA, GREECE, 2011.
- [3] C. Diakaki, "Intergrated control of traffic flow in corridor networks" Chania, Greece, 1999.
- [4] M. KONTORINAKI, "Advanced Nonlinear Control Concepts for," Chania, 2017.
- [5] I. A. Messmer, "METANET," Techical University of Crete, Dynamic Systems and Simulation Laboratory, 2007, p. 172.
- [6] R. M. Murray, "LQR Control," 2006.
- [7] V. K. Serge Hoogendoorn, "Traffic flow theory and modelling".
- [8] M. P. Christina Diakaki, "Design and Simulation test of coordinated ramp metering control (METALINE) for A-10 west in Amsterdam" Chania, 1994.
- [9] Y. Wang, M. Papageorgiou, J. Gaffney, I. Papamichail and J. Guo, "Local ramp metering in the presence of random-location bottlenecks downstream of a metered on-ramp," in *13th International IEEE Conference on Intelligent Transportation Systems*, 2010.
- [10] Y. Wang, E. B. Kosmatopoulos, M. Papageorgiou and I. Papamichail, "Local Ramp Metering in the Presence of a Distant Downstream Bottleneck: Theoretical Analysis and Simulation Study," *IEEE Transactions on Intelligent Transportation Systems*, vol. 15, no. 5, pp. 2024-2039, 10 2014.
- [11] A. Spiliopoulou, M. Kontorinaki, M. Papageorgiou and P. Kopelias, "Macroscopic traffic flow model validation at congested freeway off-ramp areas," *Transportation Research Part C: Emerging Technologies*, vol. 41, pp. 18-29, 1 4 2014.
- [12] E. Smaragdis and M. Papageorgiou, "Series of New Local Ramp Metering Strategies: Emmanouil Smaragdis and Markos Papageorgiou," *Transportation Research Record: Journal of the Transportation Research Board*, vol. 1856, pp. 74-86, 1 2003.
- [13] E. Smaragdis, M. Papageorgiou and E. Kosmatopoulos, "A flow-maximizing adaptive local ramp metering strategy," *Transportation Research Part B: Methodological*, vol. 38, no. 3, pp. 251-270, 3 2004.
- [14] P. I. Richards, *Shock Waves on the Highway*, vol. 4, INFORMS, pp. 42-51.
- [15] M. Papageorgiou and I. Papamichail, "Overview of Traffic Signal Operation Policies for Ramp Metering," *Transportation Research Record: Journal of the Transportation Research Board*, vol. 2047, no. 1, pp. 28-36, 22 1 2008.
- [16] M. Papageorgiou, "Overview of Road Traffic Control Strategies," *IFAC Proceedings Volumes*, vol. 37, no. 19, pp. 29-40, 10 2004.

- [17] M. Papageorgiou, C. Kiakaki, V. Dinopoulou, A. Kotsialos and Yibing Wang, "Review of road traffic control strategies," *Proceedings of the IEEE*, vol. 91, no. 12, pp. 2043-2067, 12 2003.
- [18] M. Papageorgiou and A. Kotsialos, "Freeway ramp metering: an overview," *IEEE Transactions on Intelligent Transportation Systems*, vol. 3, no. 4, pp. 271-281, 12 2002.
- [19] M. Papageorgiou, H. Hadj-Salem and F. Middelham, "ALINEA Local Ramp Metering: Summary of Field Results," *Transportation Research Record: Journal of the Transportation Research Board*, vol. 1603, pp. 90-98, 1 1997.
- [20] A. Michel, K. Wang and B. Hu, *Qualitative Theory of Dynamical Systems*, CRC Press, 2001.
- [21] T. Luspay, B. Kulcsár and T. Péni, "Set-theoretic analysis of the isolated ramp metering problem," *International Journal of Robust and Nonlinear Control*, vol. 26, no. 6, pp. 1246-1266, 1 4 2016.
- [22] M. J. Lighthill and G. B. Whitham, "On Kinematic Waves. II. A Theory of Traffic Flow on Long Crowded Roads," *Proceedings of the Royal Society A: Mathematical, Physical and Engineering Sciences*, vol. 229, no. 1178, pp. 317-345, 10 5 1955.
- [23] A. Kotsialos and M. Papageorgiou, "Motorway network traffic control systems," *European Journal of Operational Research*, vol. 152, no. 2, pp. 321-333, 16 1 2004.
- [24] M. Kontorinaki, I. Karafyllis, M. Papageorgiou and Y. Wang, "An adaptive control scheme for local and coordinated ramp metering," in *2017 IEEE 20th International Conference on Intelligent Transportation Systems (ITSC)*, 2017.
- [25] Y. Kan, Y. Wang, M. Papageorgiou and I. Papamichail, "Local ramp metering with distant downstream bottlenecks: A comparative study," *Transportation Research Part C: Emerging Technologies*, vol. 62, pp. 149-170, 1 2016.
- [26] Institute of Electrical and Electronics Engineers., IEEE Intelligent Transportation Systems Council and IEEE ITSS, *IEEE transactions on intelligent transportation systems.*, Institute of Electrical and Electronics Engineers, 2000.
- [27] Z. Hou, J.-X. Xu and J. Yan, "An iterative learning approach for density control of freeway traffic flow via ramp metering," *Transportation Research Part C: Emerging Technologies*, vol. 16, no. 1, pp. 71-97, 2 2008.
- [28] B. Haut, G. Bastin and Y. Chitour, "A Macroscopic traffic model for road networks with a representation of the capacity drop phenomenon at the junctions" *IFAC Proceedings Volumes*, vol. 38, no. 1, pp. 114-119, 1 1 2005.
- [29] Y. Han, A. Hegyi, Y. Yuan, S. Hoogendoorn, M. Papageorgiou and C. Roncoli, "Resolving freeway jam waves by discrete first-order model-based predictive control of variable speed limits," *Transportation Research Part C: Emerging Technologies*, vol. 77, pp. 405-420, 1 4 2017.
- [30] Dr.-Ing. A. Messmer, "METANET: A Simulation Program for motorway networks" p. 174, 2012.

- [31] R. C. Carlson, I. Papamichail and M. Papageorgiou, "Local Feedback-Based Mainstream Traffic Flow Control on Motorways Using Variable Speed Limits," *IEEE Transactions on Intelligent Transportation Systems*, vol. 12, no. 4, pp. 1261-1276, 12 2011.